A Broad-Band U-Slot Rectangular Patch Antenna on a Microwave Substrate

Kin-Fai Tong, Kwai-Man Luk, *Senior Member, IEEE*, Kai-Fong Lee, *Fellow, IEEE*, and Richard Q. Lee

***Abstract*—A broad-band U-slot rectangular patch antenna printed on a microwave substrate is investigated. The dielectric constant of the substrate is 2.33. The antenna is fed by a coaxial probe. The characteristics of the U-slot patch antenna are analyzed by the finite-difference time-domain (FDTD) method. Experimental results for the input impedance and radiation patterns are obtained and compared with numerical results. The maximum impedance bandwidth achieved is 27%, centered around 3.1 GHz, with good pattern characteristics.**

***Index Terms*—Broad-band antennas, printed antennas.**

I. Introduction

RECENTLY, a single-layer single-patch wide-band microstrip antenna in the form of a rectangular patch with a U-shaped slot has been studied [1]–[3]. The antenna was fabricated on a foam material. Impedance bandwidth of over 30%, with good pattern characteristics was obtained. Unlike most of the bandwidth enhancement methods reported in the literature, this antenna retains the major advantage of microstrip antennas—low profile.

However, it is awkward to fabricate the resonating patch on a foam material. In this paper, rectangular U-slot patch antennas printed on conventional microwave substrates using printed circuit board (PCB) fabrication technique will be investigated experimentally. FDTD codes are written to verify the experimental results. Key issues when designing broad-band U-slot patch antenna on a microwave substrate will be addressed. The geometry of a U-slot rectangular patch antenna etched on a finite grounded microwave substrate is shown in Fig. 1. The input impedance, resonant frequency and far-field radiation pattern of the antennas will be analyzed by using the three-dimensional (3-D) FDTD method, which is most suitable for this complex structure. The FDTD method requires relatively large computational and storage resources. However, these requirements are colaguately met by the processing power of the latest pc's and workstations.

The FDTD algorithm of solving the problem will be described briefly in Section II. Appropriate absorbing boundary conditions (ABC's) for terminating the computation domain will be discussed. A thin-wire approximation for the probe feed will be used to reduce the program memory requirement. Thereafter, the calculation of input impedance of the antennas, the surface current on the patch and the radiation patterns of the antennas at different operating frequencies will be described.

Manuscript received September 14, 1998; revised January 4, 2000. This work was supported by CERG Grant 9 040 210, Hong Kong.

K.-F. Tong and K.-M. Luk are with the Department of Electronic Engineering, City University of Hong Kong, Kowloon, Hong Kong.

K.-F. Lee is with the Department of Electrical Engineering, University of Missouri Columbia, Columbia, MO 65211 USA.

R. Q. Lee is with the NASA Lewis Research Center, Cleveland, OH 44135–3191 USA.

Publisher Item Identifier S 0018-926X(00)05791-4.

II. Theory

The FDTD algorithm solves Maxwell's time-dependent curl equations by first filling up the computation space with a number of "Yee" cells [4]. The relative spatial arrangement of the E and H fields on each "Yee" cell enables the conversion of Maxwell's equations into a set of finite-difference equations. These equations are then solved in a time-marching sequence by alternately calculating the electric and magnetic fields in an interlaced spatial grid.

When calculating the tangential electric fields lying on the boundary of different material, special consideration should be taken. Suppose there is an interface lying in the y-z plane between two different dielectric materials with parameters $(\sigma_1, \varepsilon_1)$ and $(\sigma_2, \varepsilon_2)$ respectively. It can be shown that E_y and E_z can be solved by (1) and (2)

$$\frac{\sigma_1+\sigma_2}{2}E_y+\frac{\varepsilon_1+\varepsilon_2}{2}\frac{\partial E_y}{\partial t}=\frac{\partial H_x}{\partial z}-\frac{\Delta H_z}{\Delta x} \quad (1)$$

$$\frac{\sigma_1+\sigma_2}{2}E_z+\frac{\varepsilon_1+\varepsilon_2}{2}\frac{\partial E_z}{\partial t}=\frac{\partial H_y}{\partial x}-\frac{\Delta H_x}{\Delta y}. \quad (2)$$

Hence, the interfaces between different dielectric materials in the FDTD simulation are handled by substituting the average values for the parameters of the materials involved.

Absorbing boundary conditions (ABC's) for mesh termination are required in the simulation. The ABC's developed by Engquist and Majda [5] are employed. The Engquist–Majda ABC's numerically absorb impinging scattered waves when applied to the outer boundary of a FDTD grid. A simplified feed model based on thin wire approximation is used to reduce program memory requirement [6], [7]. A Gaussian pulse type of voltage excitation is selected so that the frequency dependent characteristics can be obtained in one analysis cycle. The current flowing into the antenna is obtained by performing the line integral of the magnetic fields around the base of the probe at each time step. The input impedance of the antenna is determined by the ratio of the discrete Fourier transform (DFT) of the input voltage wave and that of the input current wave. The surface current density [8] on the U-slot patch is computed by the H field at a half-space step above and below the patch, which is located on the grids for the E field.

A near-to-far-field transform can be employed to obtain the far-field radiation pattern. The transformation is based on the field equivalence principle and can be performed either in the

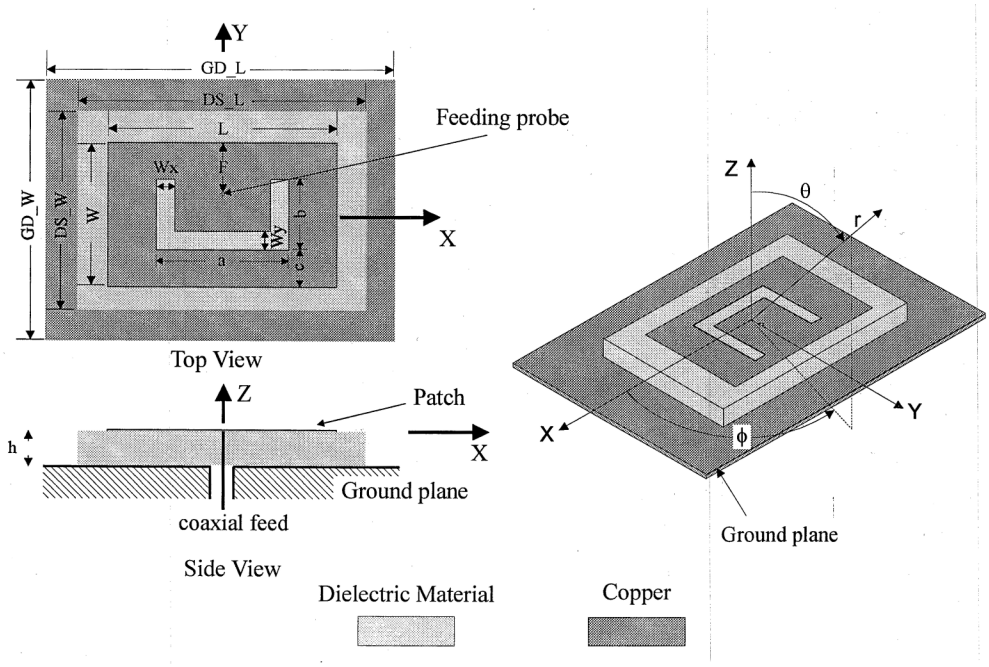

Fig. 1. Geometry of a U-slot rectangular patch antenna printed on a microwave substrate.

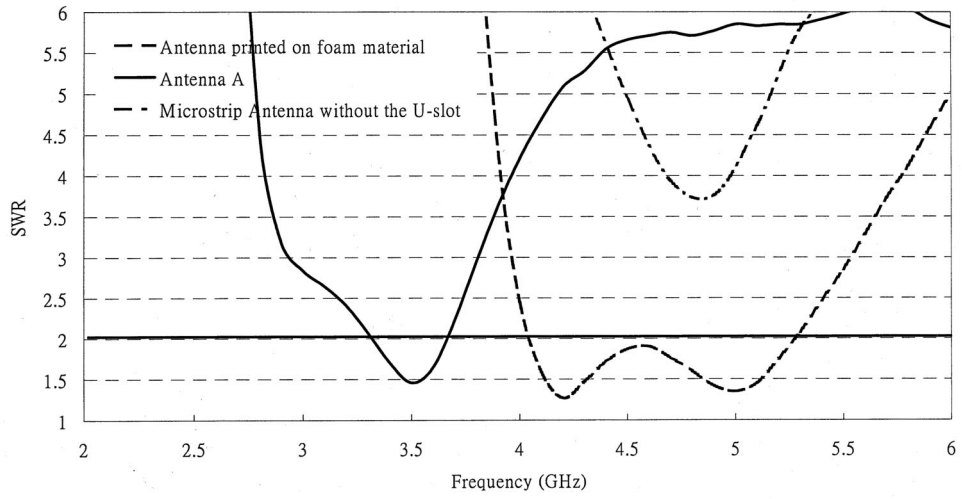

Fig. 2. Comparison of bandwidth between Antenna A and an antenna printed on foam material.

TABLE I
DIMENSIONS OF ANTENNA A, ANTENNA B, AND ANTENNA C IN MILLIMETERS

	GD_L	GD_W	DS_L	DS_W	ε_r	L	W
Antenna A	120.0	100.0	90.0	80.0	2.33	36.0	26.0
Antenna B	120.0	100.0	90.0	80.0	2.33	36.0	26.0
Antenna C	120.0	100.0	90.0	80.0	2.33	36.0	26.0
	a	b	c	h	F	w_x	w_y
Antenna A	14.0	18.0	4.0	5.0	13.0	2.0	2.0
Antenna B	14.0	18.0	4.0	6.4	13.0	2.0	2.0
Antenna C	14.0	18.0	4.0	8.0	13.0	2.0	2.0

frequency domain [9] or in the time domain [10]. According to the field equivalence principle, the electromagnetic fields outside an imaginary closed surface (a virtual surface) surrounding the object of interest can be obtained if the equivalent sources on the closed surface are known. In this paper, the equivalent sources are transformed to the frequency domain using the discrete Fourier transform. Then the near-to-far-field transformation is carried out in the frequency domain at each frequency of interest. This method can save the memory space required for the calculation.

III. RESULTS AND DISCUSSION

The U-slot rectangular patch antenna shown in Fig. 1 with dimensions tabulated in Table I (Antenna A) is investigated first.

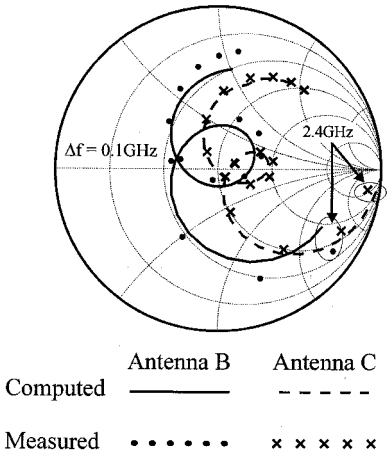

Fig. 3. Computed and measured impedances of Antenna B and Antenna C.

TABLE II
OPERATING FREQUENCIES AND BANDWIDTH OF ANTENNA B

Antenna B	f_l (GHz)	f_o (GHz)	f_u (GHz)	BW (GHz)	%BW (%)
Computed	2.87	3.28	3.69	0.82	25.0
Measured	2.76	3.16	3.56	0.80	25.3

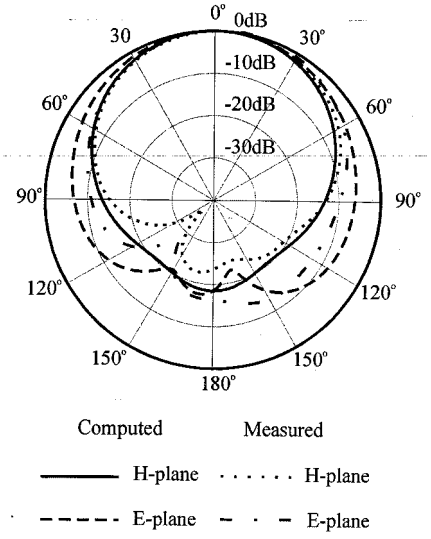

Fig. 4. Radiation patterns of Antenna B operated at 2.76 GHz.

The FDTD code developed by the authors includes the effect caused by a ground plane of finite size.

The space steps in the x- and y-directions Δx and Δy used in the FDTD simulation are first determined from the smallest parameter of the antenna structure, which is the width of the U-slot, w_x, and w_y. Then, the space steps in the z-direction are based on Δx. For Antenna A, the dimensions of the space steps are $\Delta x = 1.0$ mm, $\Delta y = 1.0$ mm, and $\Delta z = 0.83$ mm and Δz equal 0.89 and 0.91 mm in modeling Antenna B and C, respectively.

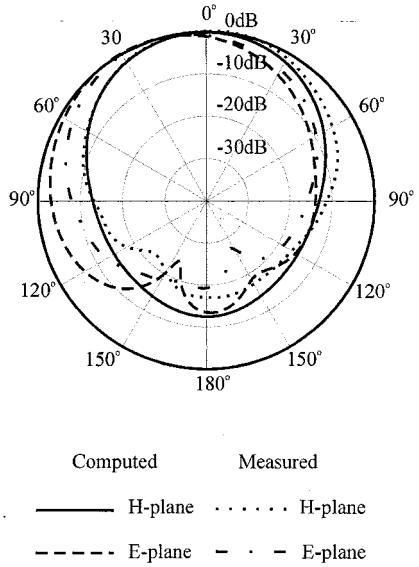

Fig. 5. Radiation patterns of Antenna B operated at 3.56 GHz.

The time step used is $\Delta t = 1.60$ ps, such that the Courant stability condition is satisfied. The size of the computational domain is $180\Delta x \times 160\Delta y \times 66\Delta z$. The number of space steps between the antenna and the ABC's is 30 steps in all directions. The simulation is performed for 20 000 time steps to allow the input response to drop to an insignificant value.

The gap-voltage model together with Jensen's model [11] are used to simulate the probe feeding configuration. The Gaussian pulse of the form $g(t) = e^{-(t-t_0)^2/T^2}$, parameters $T = 0.9369$ ns, and $t_o = 5T = 4.6845$ ns, are used. The 3-dB bandwidth of the pulse is about 2 GHz. The Gaussian pulse will have a value of e^{-25} or almost 220 dB down from the maximum value at the time of truncation at $t = 0$ and $t = 2t_o$.

The dimensions of Antenna A were based on the antenna designed on foam material [3, with $a = 12$ mm and $b = 20$ mm]. First, the dimensions of the U-shaped slot were adjusted to obtain a good impedance matching. Although the desired impedance was obtained, the impedance bandwidth of the antenna was less than 10%. The SWR against frequency plot of Antenna A, the antenna printed on foam material [3] and microstrip antenna without the U-slot are shown in Fig. 2 for comparison. The decrease of the bandwidth can be explained by the increase of quality factor Q of the antenna due to the use of the microwave substrate.

As microwave substrate of lower dielectric constant substrate is not available, the only way to reduce the Q factor is to increase the thickness of the substrate. A testing antenna (Antenna B) with a thicker substrate was designed.

The computed and measured values of the impedance of Antenna B are shown in Fig. 3. It can been calculated that the percentage bandwidth is about 25%. The agreement between the computed and measured results is good. The center frequency (f_o), upper cutoff frequency (f_u), lower cutoff frequency (f_l), the absolute bandwidth (BW) and percentage bandwidth (percentage BW) are tabulated in Table II for reference.

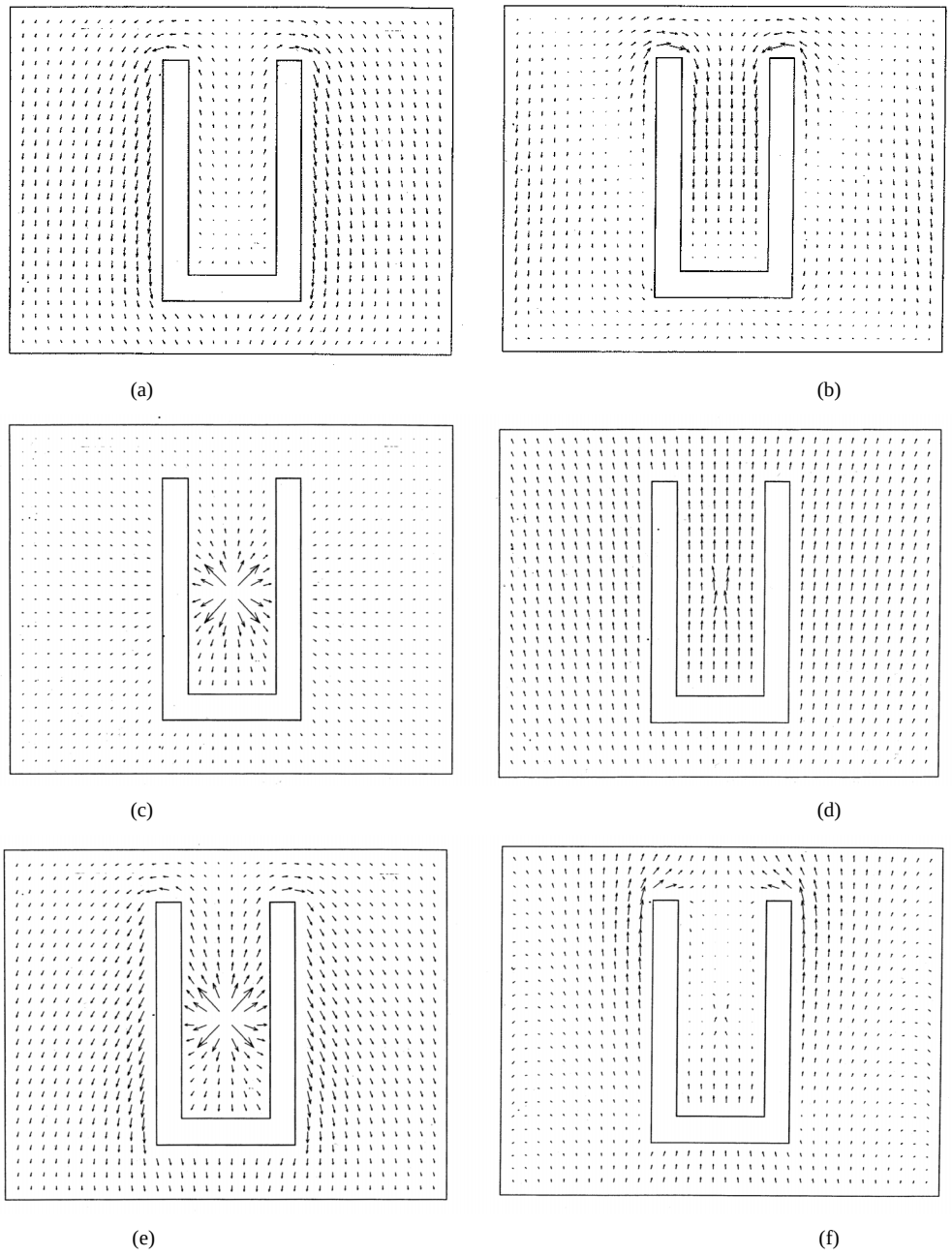

Fig. 6. The surface current density of Antenna B at 3.30 GHz. (a) On the upper side of the metal patch—real part. (b) On the upper side of the metal patch—imaginary part. (c) On the lower side of the metal patch—real part. (d) On the lower side of the metal patch—imaginary part. (e) The sum of the current density on the upper and lower sides—real part. (f) The sum of the current density on the upper and lower sides—imaginary part.

Then, the far-field radiation of Antenna B was studied. In Figs. 4 and 5, the H-plane and E-plane radiation patterns are shown. We can see that the H-plane radiation pattern is symmetrical with respect to the x-axis, but not for the E-plane radiation pattern. This may be due to the existence of the U-slot. Moreover, when the position of the U-slot is varied, the impedance of the U-slot antennas will also be affected and the bandwidth of the antenna will be decreased. The 3-dB beamwidth of both the E and H planes are listed in Table III. We can see that there is reasonably good agreement between the computed and measured results. It should be mentioned that the front-to-back ratio is defined by the IEEE standard [12].

TABLE III
FAR-FIELD CHARACTERISTICS OF ANTENNA B AT 2.76 GHz AND 3.56 GHz

		3 dB beamwidth (degree)		front-to-back ratio (dB)	
		H-plane	E-plane	H-plane	E-plane
2.76 GHz	computed	79°	99°	19.17	16.67
	measured	79°	85°	19.17	18.88
3.56 GHz	computed	70°	98°	14.17	12.92
	measured	70°	77°	15.88	19.58

Finally, the surface current density distribution of Antenna B is investigated. The surface current density, J_s, on the metal patch, is calculated by the H field at a half space step above and below the metal patch. The surface current density distribu-

TABLE IV
OPERATING FREQUENCIES AND BANDWIDTH ANTENNA C

Antenna C	f_l (GHz)	f_o (GHz)	f_u (GHz)	BW (GHz)	%BW (%)
Computed	2.72	3.14	3.56	0.84	26.8
Measured	2.68	3.09	3.50	0.82	26.5

tion of the Antenna B operated at 3.3 GHz is shown in Fig. 6. Solid lines are used to show the rectangular patch and the U-slot. When the antenna operates at the resonant frequency, the current density that flows on the upper surface of the metal surface circulates around the arm of the U-slot and flows to the base of the U-slot. And the amplitude of the current are relatively smaller than that of the lower surface. On the lower surface of the metal patch, the real part of the current density depends on the position of the coaxial probe, a relatively strong current spreading radically from the feeding point. The resonant mode of the antenna can be observed from the imaginary part of the current density. Moreover, the magnitude of the current is negligible out of resonance.

One of the reasons which makes the U-slot patch antennas exhibit broad-band characteristic is the low Q-factor of these antennas. A thicker antenna substrate, h, will produce a lower Q-factor. A higher h/λ_g ratio of 0.12 was used for the second design (Antenna C). The impedance bandwidth $(\mathrm{SWR} < 2)$ of the Antenna C is about 27%. The dimensions of Antenna C are also listed in Table I.

The comparison between the computed and measured impedance of Antenna C is shown in Fig. 3. We can see that the agreement is good. The discrepancy of the center frequency between the computed and measured results is about 3.6%. It may be caused by the thin-wire approximation made in the feed model and the ABC's used for the mesh termination. For a more accurate and effective simulation, resistive source [13] and the perfectly matched layer [14] can be better modeling methods. The center frequency (f_o), upper cutoff frequency (f_u), lower cutoff frequency (f_l) and bandwidth of Antenna C are listed in Table IV. In Figs. 7 and 8, the computed and measured results of the radiation pattern of Antenna C operated at the upper and lower cutoff frequencies are shown. Reasonably good agreement can be observed from these figures. The 3-dB beamwidth and front-to-back ratio are tabulated in Table V.

The measured gain of Antenna B and Antenna C are shown in Fig. 9. We can see that the gain of each antenna is about 6.5 dB, which is less than the case with a foam substrate (8.5 dB). When the antennas operate at a higher frequency, the gain of the antennas drop. This drop is more serious in Antenna C and may be caused by surface waves, since a larger thickness was used in Antenna C.

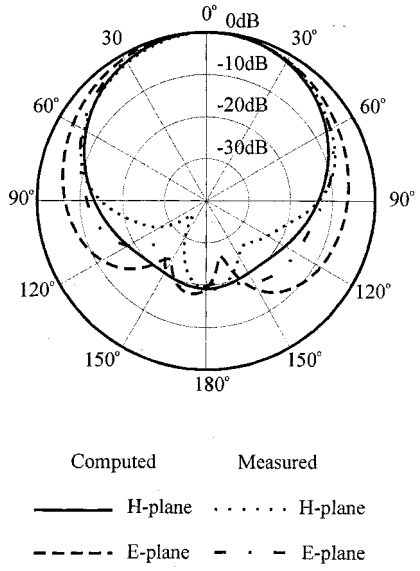

Fig. 7. Radiation patterns of Antenna C operated at 2.68 GHz.

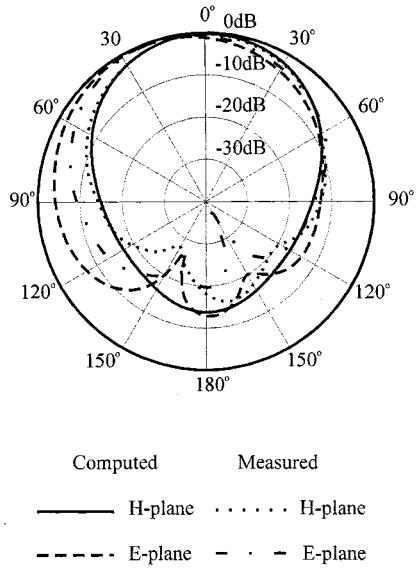

Fig. 8. Radiation patterns of Antenna C operated at 3.50 GHz.

TABLE V
FAR-FIELD CHARACTERISTICS OF ANTENNA C AT 2.68 GHz AND 3.50 GHz

		3 dB beamwidth (degree)		front-to-back ratio (dB)	
		H-plane	E-plane	H-plane	E-plane
2.68 GHz	computed	79°	97°	22.27	17.72
	measured	79°	85°	18.18	16.82
3.50 GHz	computed	74°	100°	12.69	12.69
	measured	78°	79°	16.92	19.23

IV. CONCLUSION

This paper has presented a new design of broad-band U-slot rectangular patch antenna printed on a microwave substrate. The analysis is based on the 3-D FDTD method. The foam material in the previous studies is replaced by a dielectric substrate of $\varepsilon_r = 2.33$. This substitution can ease the fabrication of the antennas especially in an array environment, since conventional

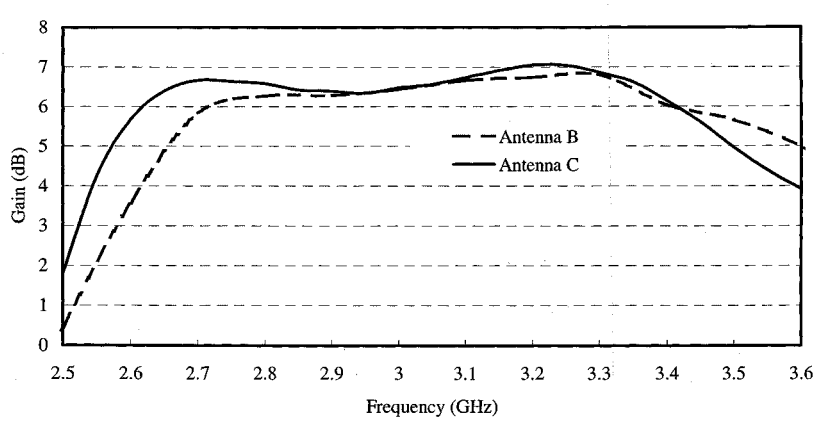

Fig. 9. Measured gains of Antenna B and Antenna C.

PCB fabrication technique can be used. It is found that the crucial step to design a broad-band U-slot patch antenna printed on a microwave substrate is to use a larger thickness than the case with a foam material. The achieved impedance bandwidth of the U-slot patch antennas on microwave substrates are 25% and 27% with h/λ_g equal to 0.1 and 0.12, respectively. The computed resonant frequencies and far-field patterns agree well with measured data. The measured gain of each antenna is about 6.5 dB.

REFERENCES

[1] T. Huynh and K. F. Lee, "Single-layer single-patch wideband microstrip antenna," *Electron. Lett.*, vol. 31, no. 16, pp. 1310–1312, 1995.

[2] K. F. Lee, K. M. Luk, K. F. Tong, Y. L. Yung, and T. Huynh, "Experimental study of a two-element array of U-slot patches," *Electron. Lett.*, vol. 32, no. 5, pp. 418–420, 1996.

[3] K. F. Lee, K. M. Luk, K. F. Tong, S. M. Shum, T. Huynh, and R. Q. Lee, "Experimental and simulation studies of coaxially fed U-slot rectangular patch antenna," *Inst. Elect. Eng. Proc. Microwave Antennas Propagat.*, vol. 144, no. 5, Oct. 1997.

[4] K. S. Yee, "Numerical solution of initial boundary value problems involving Maxwell's equations in isotropic media," *IEEE Trans. Antennas Propagat.*, vol. AP-14, pp. 302–307, Mar. 1966.

[5] B. Engquist and A. Majda, "Absorbing boundary conditions for the numerical simulation of waves," *Math. Computat.*, vol. 31, pp. 629–651, 1977.

[6] R. J. Luebbers, L. Chen, T. Uno, and S. Adachi, "FDTD calculation of radiation patterns, impedance, and gain for a monopole antenna on a conducting box," *IEEE Trans. Antennas Propagat.*, vol. 40, pp. 1577–1583, Dec. 1992.

[7] P. A. Tirkas and C. A. Balanis, "Finite difference time domain method for antenna radiation," *IEEE Trans. Antennas Propagat.*, vol. 40, pp. 334–340, Mar. 1992.

[8] S. Maci, G. Biffi Gentili, P. Piazzesi, and C. Salvador, "Dual-band slot-loaded patch antenna," *Inst. Elect. Eng. Proc. Microwaves Antennas Propagat.*, vol. 142, no. 3, 1995.

[9] K. S. Yee, D. Ingham, and K. Shlager, "Time-domain extrapolation to the far field based on FDTD calculations," *IEEE Trans. Antennas Propagat.*, vol. 39, pp. 410–413, Mar. 1991.

[10] R. J. Luebbers, K. Kunz, M. Schneider, and F. Hunsberger, "A finite-difference time-domain near zone to far zone transformation," *IEEE Trans. Antennas Propagat.*, vol. 39, pp. 429–433, Apr. 1991.

[11] M. A. Jensen and Y. Rahmat-Samii, "Performance analysis of antenna for hand transceiver using FDTD," *IEEE Trans. Antenna Propagat.*, vol. 42, pp. 1106–1113, Aug. 1994.

[12] "IEEE standard definitions of terms for antennas," *IEEE Trans. Antennas Propagat.*, pt. II, vol. AP-31, p. 15, Nov. 1983.

[13] R. J. Luebbers, "A simple feed model that reduces time steps needed for FDTD antenna and microstrip calculations," *IEEE Trans. Antennas Propagat.*, vol. 44, pp. 1000–1005, July 1996.

[14] J. Berenger, "A perfectly matched layer for the absorption of electromagnetic waves," *J. Comput. Phys.*, vol. 114, pp. 185–200, Oct. 1994.

Kin-Fai Tong (M'99) was born in Hong Kong in 1970. He received the B.Eng. and Ph.D. degrees in electronic engineering from the City University of Hong Kong, in 1993 and 1997, respectively.

In 1993, he joined the Department of Electronic Engineering, City University of Hong Kong, as a Research Assistant. He is currently a Research Fellow there. His research interests include design of microstrip antenna and mircowave measurement.

Kwai-Man Luk (S'80-M'86-SM'94) was born in Hong Kong. He received the B.Sc. (Eng.) and Ph.D. degrees in electrical engineering from The University of Hong Kong, in 1981 and 1985, respectively.

In 1985, he joined the Department of Electronic Engineering, City University of Hong Kong, as a Lecturer. Two years later, he moved to the Department of Electronic Engineering, The Chinese University of Hong Kong, where he spent four years. He returned to City University of Hong Kong in 1992 where he is currently Professor (Chair) of Electronic Engineering and the Director of the Wireless Communications Laboratory. His postgraduate studies were on Gaussian beam wave theory and microwave open resonators and their applications. He is the author of four research book chapters, 128 journal papers and 108 conference papers. His recent research interests include design of microstrip, planar and dielectric resonator antennas, microwave measurements, computational electromagnetics.

Dr. Luk was the Technical Program Chairperson of the Progress in Electromagnetics Research Symposium (PIERS 1997) held in Hong Kong, January 1997, and the General Vice-Chairperson of the 1997 Asia-Pacific Microwave Conference held in Hong Kong, December 1997. He received the International Best Paper Award and the Japan Microwave Prize at the 1994 Asia Pacific Microwave Conference, Chiba, Japan, in December 1994. He completed CERG project (rated excellent) in 1995. He is a Fellow of the Chinese Institute of Electronics and the IEE and a member of the Electromagnetics Academy.

Kai-Fong Lee (M'73, SM'76-F'97) received the B.Sc. and M.Sc. degrees from Queen's University, Ottawa, Canada, in 1961 and 1963, respectively, and the Ph.D. degree from Cornell University, Ithaca, NY, in 1966, all in electrical engineering.

He held research appointments at University of California, San Diego (1966–1967), the National Center for Atmospheric Research (1968–1969), National Oceanic and Atmospheric Administration (1972–1973), UCLA (summer 1975) and NASA (summers 1986, 1987). He was an Assistant/Associate Professor at the Catholic University of America, Washington, DC (1967–1972), a Lecturer/Senior Lecturer/Reader at The Chinese University of Hong Kong (1973–1984), and a Professor at The University of Akron, OH (1985–1988). He was the founding Head of the Department of Electronic Engineering, City University of Hong Kong (1984–1985). He served as Professor and Chairman of the Department of Electrical Engineering at The University of Toledo, OH, from 1988 to 1995. Since January 1996 he has been Chairman and LaPierre Professor of the Department of Electrical Engineering, University of Missouri-Columbia. He worked on plasma waves and instabilities from 1965 to 1980 and on antennas since 1981. His publications include a textbook *Principles of Antenna Theory* (New York: Wiley, 1984), an edited book *Advances in Microstrip and Printed Antennas* (New York: Wiley, 1997), several invited book chapters on microstrip antennas, 130 journal articles, and 100 conference papers.

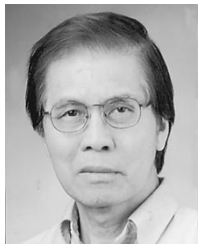

Richard Q. Lee received the B.S. and M.S. degrees in electrical engineering from the University of Illinois, Urbana-Champaign, in 1964 and 1966, respectively, and the Ph.D. in electrical engineering from Michigan State University, East Lansing, in 1970.

Since 1980, he was with NASA Glenn Research Center, Cleveland, OH, involved in the technology development of printed circuit antennas and MMIC phased arrays for satellite communications applications. Currently, he is a Senior Research Engineer with the RF Technology Branch of the Space Communications Division, NASA Glenn Research Center. He is the author or coauthor of 138 journal and conference papers and two book chapters on printed antennas. Also, he is the coinventor of a patent on optically transparent printed antennas.